Nanoscale Res Lett (2010) 5:108–115
DOI 10.1007/s11671-009-9451-2

NANO EXPRESS

Interaction Between Nano-Anatase TiO_2 and Liver DNA from Mice In Vivo

Na Li · Linglan Ma · Jue Wang · Lei Zheng · Jie Liu · Yanmei Duan · Huiting Liu · Xiaoyang Zhao · Sisi Wang · Han Wang · Fashui Hong · Yaning Xie

Received: 14 August 2009 / Accepted: 24 September 2009 / Published online: 13 October 2009

Abstract Nano-TiO_2 was shown to cause various toxic effects in both rats and mice; however, the molecular mechanism by which TiO_2 exerts its toxicity is poorly understood. In this report, an interaction of nano-anatase TiO_2 with liver DNA from ICR mice was systematically studied in vivo using ICP-MS, various spectral methods and gel electrophoresis. We found that the liver weights of the mice treated with higher amounts of nano-anatase TiO_2 were significantly increased. Nano-anatase TiO_2 could be accumulated in liver DNA by inserting itself into DNA base pairs or binding to DNA nucleotide that bound with three oxygen or nitrogen atoms and two phosphorous atoms of DNA with the Ti–O(N) and Ti–P bond lengths of 1.87 and 2.38 Å, respectively, and alter the conformation of DNA. And gel electrophoresis showed that higher dose of nano-anatase TiO_2 could cause liver DNA cleavage in mice.

Keywords Nano-anatase TiO_2 · Mice · DNA · Binding information · DNA cleavage

Introduction

Titanium dioxide (TiO_2), a natural nonsilicate mineraloxide, occurs in different forms and is widely used in the cosmetics, pharmaceutical and paint industries as a coloring material because of its high stability, anticorrosion and photocatalysis. With the small size and large surface area, nanoparticles can be an active group or exert intrinsic toxicity. However, the widespread use of nano-TiO_2 and its potential entry through dermal, ingestion and inhalation routes suggest that nanosize TiO_2 could result in human health risk. Many in vivo studies showed that nanomaterial particles can be accumulated in the liver, kidney, spleen, lung, heart and brain, whereby generating various inflammatory responses [1–8]. For instance, nanomaterial particles can promote enzymatic activities and the mRNA expression of cytokines during proinflammatory responses in rats and mice [4–10]. Nanoparticles also can produce reactive oxygen [11] and cause DNA cleavage in cells [12]. A wide range of biological and biochemical effects of nanomaterials might be resulted from the direct or indirect interaction of nano-anatase TiO_2 with DNA. Numerous in vitro studies reported that indirect interaction is associated with oxidative damage to DNA, thereby increasing cellular oxidants in the cells and producing free radicals and 8-oxo-7, 8-dihydro-2 *-deoxyguanosine (8-oxodG) and 8-hydroxydeoxy adenosine (A8OH·) that result in DNA cleavage under UVA illumination [11–16]. Conversely, direct interaction involves covalent binding between nano-anatase TiO_2 and DNA. However, little is known about evidence for interaction of nano-anatase TiO_2 with DNA in vivo and particularly the effect of nano-anatase TiO_2 on the DNA structure and cell apoptosis in vivo. In an effort to investigate various interactions between nano-anatase TiO_2 and DNA in vivo, including covalent binding of nano-anatase

Na Li, Linglan Ma, Jue Wang and Lei Zheng contributed equally to this work.

N. Li · L. Ma · J. Wang · L. Zheng · J. Liu · Y. Duan · H. Liu · X. Zhao · S. Wang · H. Wang · F. Hong (✉)
Medical College of Soochow University, 215123 Suzhou, People's Republic of China
e-mail: Hongfsh_cn@sina.com

Y. Xie
Synchrotron Radiation Laboratory, Institute of High Energy Physics, The Chinese Academy of Science, 100039 Beijing, People's Republic of China

TiO_2 to DNA, the structure of DNA, DNA integrity and cell apoptosis, we used different techniques to examine mice liver DNA treated with various doses of nano-anatase TiO_2. Our findings will provide an important theoretical basis for evaluating the toxicity underlying effects of nanomaterials on animals and human.

Materials and Methods

Chemicals and Preparation

Nano-anatase TiO_2 was prepared via controlled hydrolysis of titanium tetrabutoxide as described previously [17]. Briefly, colloidal titanium dioxide was prepared via controlled hydrolysis of titanium tetrabutoxide. In a typical experiment, 1 ml of $Ti(OC_4H_9)_4$ dissolved in 20 ml of anhydrous isopropanol was added dropwise to 50 ml of double-distilled water adjusted to pH 1.5 with nitric acid under vigorous stirring at room temperature. Then, the temperature was raised to 60 °C and kept 6 h for better crystallization of nano-TiO_2 particles. The resulting translucent colloidal suspension was evaporated using a rotary evaporator yielding a nanocrystalline powder. The obtained powder was washed three times with isopropanol and dried at 50 °C until complete evaporation of the solvent. The average grain size calculated from broadening of the (101) XRD peak of anatase (Fig. 1) using Scherrer's equation was ca 5 nm. The Ti^{2+} content in the nano-anatase was measured by ICP-MS, and O, C and H contents in the nano-anatase were assayed by Elementar Analysensysteme Gmbh, showing that Ti, O, C and H weights in the nano-anatase were 58.114, 40.683, 0.232 and 0.136% in compositions, respectively.

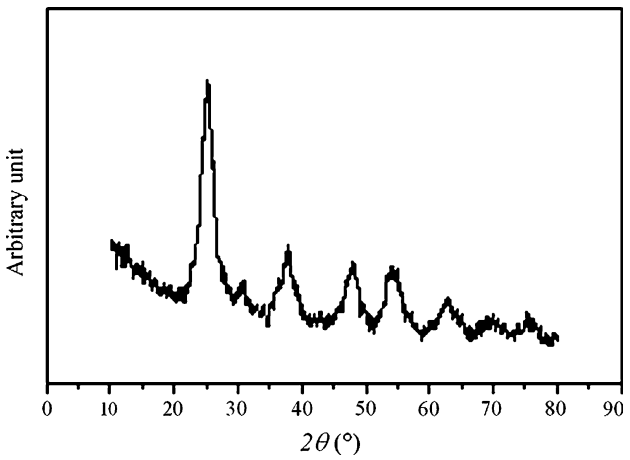

Fig. 1 The average grain size calculated from broadening of the (101) XRD peak of anatase using Scherrer's equation

A 0.5% hydroxypropylmethylcellulose K4M (HPMC, K4M) was used as a suspending agent. Nano-anatase powder was dispersed onto the surface of 0.5%, w/v HPMC, and then the suspending solutions containing the TiO_2 colloidal suspensions were treated by ultrasonic for 30 min and mechanically vibrated for 5 min.

Animals and Treatment

CD-1 (ICR) mice of 60 females (20 ± 2 g) were purchased from the Animal Center of Soochow University. Animals were housed in stainless steel cages in a ventilated animal room. Room temperature was maintained at 20 ± 2 °C, relative humidity was at 60 ± 10% and a 12-h light/dark cycle. Distilled water and sterilized food for mice were available ad libitum. They were acclimated to this environment for 5 days prior to dosing. All procedures used in animal experiments were in compliance with the Soochow University ethics committee. Animals were randomly divided into six groups: control group (treated with 0.5% HPMC) and five experimental groups. Experimental groups were injected into abdominal cavity with nano-anatase TiO_2 (5, 10, 50, 100 and 150 mg/kg body weight) everyday for 14 days, respectively. The control group was treated with 0.5% HPMC. The symptom and mortality were observed and recorded carefully everyday for 14 days. After 14 days, the body weight of all animals were weighed, and they were killed after being anaesthetized by ether. The liver was excised and washed carefully by 95% saline then weighed accurately.

After weighing the body and tissues, the coefficients of the liver to body weight were calculated as the ratio of the livers (wet weight, mg) to body weight that were expressed as milligrams (wet weight of livers)/grams (body weight) (g).

Preparation of DNA Samples from Mice Liver

The DNA was extracted from the liver and purified as described by the manufacturer (Takara company), A260/A280 (>1.8) indicated that the DNA was sufficiently free of protein. The purified DNA was resuspended in Tris–HCl buffer (pH 7.2) and then was stored at 4 °C.

Titanium Content Analysis of Liver DNA

Approximately 0.5 mg of DNA from various treated mice was digested and analyzed for titanium content. Briefly, prior to elemental analysis, the brain tissues were digested with nitric acid (ultrapure grade) overnight. After adding 0.5 ml H_2O_2, the mixed solutions were placed at 160 °C with high-pressure reaction containers in an oven chamber until the samples were completely digested. Then, the

solutions were incubated at 120 °C to remove the remaining nitric acid until the solutions were colorless and clear. Finally, the remaining solutions were diluted to 3 ml with 2% nitric acid. Inductively coupled plasma-mass spectrometry (ICP-MS, Thermo Elemental X7, Thermo Electron Co.) was used to determine the titanium concentration in the samples. Indium of 20 ng/ml was chosen as an internal standard element. The detection limit of titanium was 0.074 ng/ml. Data are expressed as nanograms per gram fresh tissue.

UV–Vis Absorption Spectroscopy

The absorption spectra of the liver DNA from various treated mice were measured from 200 to 300 nm at room temperature using UV–vis spectrophotometer (UV-3010, Hitachi, Japan). The final concentration of liver DNA was 40 μM.

Assay of Extended X-Ray Absorption Fine Structure (EXAFS) Spectroscopy

In order to detect the local coordination environment at Ti sites, Ti K-edge X-ray absorption data of the nano-anatase TiO_2-DNA from 150 mg/kg body weight nano-anatase TiO_2-treated mice were collected in fluorescence mode under liquid nitrogen temperature at the 4W1B beamline of the Beijing Synchrotron Radiation Facility (operating at dedicated mode of 2.2 GeV and 40–80 mA). A Ge(III) double-crystal monochromator was used and detuned to minimize the higher harmonic contamination at high energy region. Energies were calibrated using an internal corresponding Ti foil standard. The biological samples were placed in a cuvette and sealed with Kapton tape as transmission windows. A Lytle fluorescence detector was utilized with a Cr filter. More than five scans were recorded and averaged in order to improve the signal to noise ratio. For a given sample, no photon reduction should be observed in the first collected spectra compared with the last. The first inflection for edge of the corresponding metal foil was used for energy calibration.

The EXAFS data were extracted from the absorption spectra obtained by averaging the raw data collected over five consecutive scans and normalized by dividing the absorption spectra by the height of the edge jump. Background removal was performed by following standard procedure. The absorption threshold for a core electron excitation was selected at the inflection point in the rise of the "white-line" absorption peak. Correlations between $(E_0, \delta r_j)$ and (N_j, σ_j^2) fitting parameters were reduced by weighting the XAFS data by k^n $(n = 1, 2, 3)$. The passive electron amplitude reduction factor (S_0^2), which is assumed to depend only on the absorbing atom type and not on its environment, was obtained from its fits to those corresponding metal foil data collected under the same condition and set to this value in all other fits. The structural parameters were obtained by curve fitting the experimental data with the theoretical functions by nonlinear least squares minimization of the residuals. The data were analyzed using the EXAFSPAK analysis suite (http://www-ssrl.slac.stanford.edu/~george/exafspak/exafs.htm) together with theoretical standards from FEFF code, and the latter was used to calculate amplitude and phase shift functions [18].

DNA Assay of Circular Dichroism (CD) Spectroscopy

CD spectra of the liver DNA from various treated mice were detected from 190 to 300 nm at room temperature on a JASCO-J-810 spectropolarimeter with a quartz sample cell of an optical path length of 1 cm. The final concentration of liver DNA was 40 μM. Scanning replication of five times was done for each sample.

Analysis of Agarose Gel Electrophoresis

The integrity of the liver DNA from various treated mice was examined with agarose gel electrophoresis.

Statistical Analysis

Results were analyzed statistically by the analysis of variance (ANOVA). When analyzing the variance treatment effect ($P \leq 0.05$), the least standard deviation (LSD) test was applied to make comparison between means at the 0.05 levels of significances.

Results

Body Weight and The Coefficient of Mice Liver

During administration, all animals were at growth state. The daily behaviors such as feeding, drinking and activity in nano-anatase TiO_2-treated groups were as normal as the control group. After 14 days, the body weight (grams) was measured, and then the mice were killed, the livers were collected and weighed (milligrams). We then calculated the coefficients of the liver to body weight that were expressed as milligrams (wet weight of livers)/grams (body weight) (Table 1). While the significant differences were not observed in the coefficients of the liver in the 5 and 10 mg/kg body weight nano-anatase TiO_2 groups ($P > 0.05$), the coefficients of the liver in the 50, 100 and 150 mg/kg body weight nano-anatase TiO_2 groups were significantly higher ($P < 0.05$ or $P < 0.01$) than the control.

Table 1 The coefficient of liver of mice after abdominal cavity injected to nano-anatase TiO_2 for 2 weeks

	Nano-anatase TiO_2 (mg/kg BW)					
	Control	5	10	50	100	150
Liver/BW (mg/g)	57.03 ± 2.85	56.14 ± 2.61	59.38 ± 2.97	61.44 ± 3.07*	62.49 ± 3.12*	69.33 ± 3.47**

Ranks marked with a star or double stars mean that they are significantly different from the control (no nano-anatase TiO_2) at the 5 or 1% confidence level, respectively. Values represent means ± SE, $n = 10$

Table 2 The content of titanium accumulation in liver DNA of mice after abdominal cavity injected to nano-anatase TiO_2 for 2 weeks

	Nano-anatase TiO_2 (mg/kg BW)					
	Control	5	10	50	100	150
Ti content (ng/mg DNA)	Not detected	14.45 ± 0.72	44.36 ± 2.24*	191.05 ± 9.55**	439.83 ± 21.99**	805.64 ± 40.28**

Ranks marked with a star or double stars mean that they are significantly different from the control (no nano-anatase TiO_2) at the 5 or 1% confidence level, respectively. Values represent means ± SE, $n = 3$

Titanium Content Analysis

To obtain direct evidence for interaction of nano-anatase TiO_2 with DNA from the liver of mice, we measured the contents of titanium in purified DNA by ICP-MS (Table 2). With increasing the injection dosages of nano-anatase TiO_2, the titanium contents in the liver DNA were significantly increased, suggesting that, after entering the animals, nano-anatase TiO_2 could combine with DNA.

UV–Vis Absorption Spectra of DNA from Mice Liver

The absorption spectra of liver DNA of mice with increasing dosages of nano-anatase TiO_2 are shown in Fig. 2. Because there would be an absorbance decreasing at 260 nm upon increasing doses of nano-anatase TiO_2, we added nano-anatase TiO_2 to working and reference cells, indicating that the decrease in absorbance was not derived from the high dose of nano-anatase TiO_2, but from the interaction of nano-anatase TiO_2 with DNA. As illustrated in Fig. 2, both apparent blue shifts and significant hypochromicities were observed at 205 nm.

EXAFS of Ti^{4+}–DNA from The Mouse Liver

K edge of Ti^{4+} in nano-anatase TiO_2–DNA complex is shown in raw absorption spectrum (Fig. 3), which presents the characteristic of the strong Ti^{4+} white line. The Fourier transform for the κ^3-weighted Ti K-edge EXAFS oscillations in the range of 1–6 Å and the scattering path contributions obtained from curve fittings are shown in Fig. 4. The local structure coordination parameters obtained from the curve fitting are listed in Table 3, showing that Ti was bound with three oxygen or nitrogen atoms on DNA in its

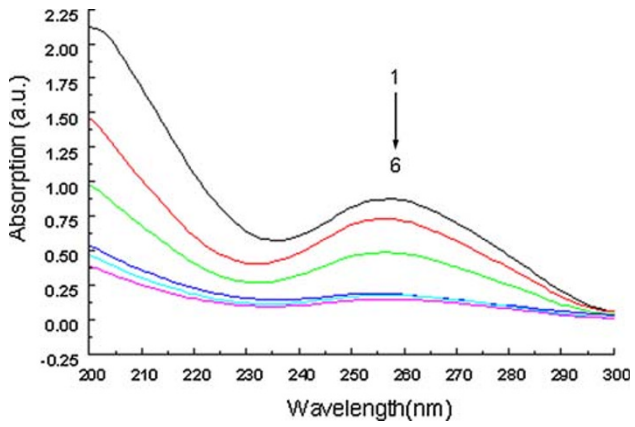

Fig. 2 Absorption spectrum of DNA of mice liver in different nano-anatase TiO_2 dose groups. *1* Control; *2* 5 mg/kg body weight nano-anatase TiO_2; *3* 10 mg/kg body weight nano-anatase TiO_2; *4* 50 mg/kg body weight nano-anatase TiO_2; *5* 100 mg/kg body weight nano-anatase TiO_2 and *6* 150 mg/kg body weight nano-anatase TiO_2

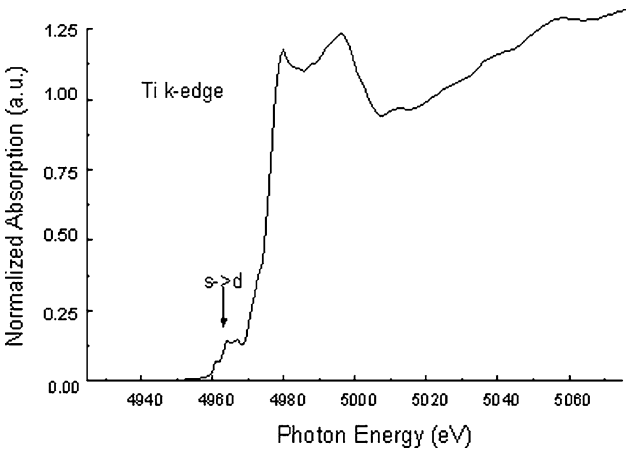

Fig. 3 Fluorescence-extended X-ray absorption fine structure spectrum of Ti^{4+} in DNA from liver of mice in 150 mg/kg body weight nano-anatase TiO_2 dose group

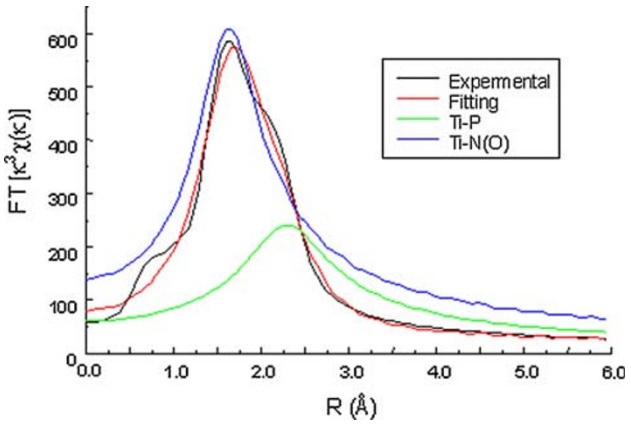

Fig. 4 Radical distribution function of Ti^{4+}in DNA from liver of mice in 150 mg/kg body weight nano-anatase TiO_2 dose group

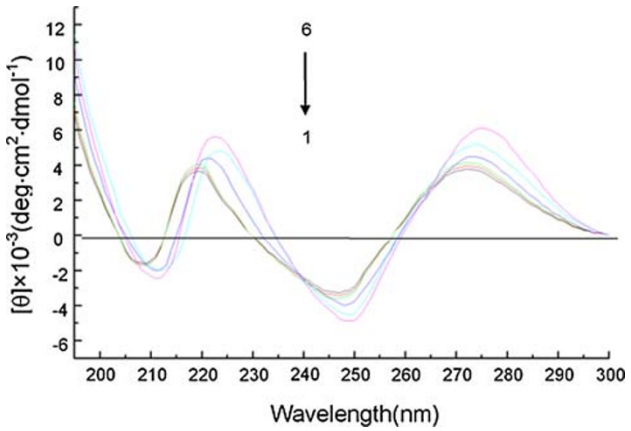

Fig. 5 Ultraviolet circular dichroism (*CD*) spectra of DNA from liver of mice in various nano-anatase TiO_2 dose groups. *1* Control; *2* 5 mg/kg body weight nano-anatase TiO_2; *3* 10 mg/kg body weight nano-anatase TiO_2; *4* 50 mg/kg body weight nano-anatase TiO_2; *5* 100 mg/kg body weight nano-anatase TiO_2 and *6* 150 mg/kg body weight nano-anatase TiO_2

Table 3 The coordination parameters obtained from curve fitting of EXAFS

Sample (fresh)	Shell	*N*	*R* (Å)	σ^2 (Å^2)	ΔE_0 (eV)
	Ti–N(O)	3	1.87	0.0029	−3.1
	Ti–P	2	2.38	0.0057	

Shell indicates the type of ligands for each shell of the fit, *N* is the coordination number, *R* is the metal-scatterer distance, σ^2 is a mean square deviation in *R* and ΔE_0 is the shift in E_0 for the theoretical scattering functions. Numbers in parentheses were not varied during optimization

The errors of data and fits are roughly estimated from the change of the residual factors to be 5% for *N*, 0.25% for *R*, 10% for σ^2 and 4 eV for ΔE_0. No ambiguities of the theoretical standards are included

first shell at the distance of the Ti–O(N) bond of 1.87 Å. The second shell at 2.38 Å was two phosphorous (P) atoms.

CD Spectra of DNA from The Mouse Liver

As shown in Fig. 5, the spectra in the 5 and 10 mg/kg body weight groups are similar to the control, indicating that DNA conformation has no obvious changes. In the 50, 100 and 150 mg/kg body weight doses of nano-anatase TiO_2, the positive bands at 220 and 272 nm increased and red shifted by 2–3 nm, and the negative bands at 210 and 244 nm decreased and red shifted by 1–2 nm, suggesting that nano-anatase TiO_2 caused the changes of DNA conformation.

Agarose Gel Electrophoresis of DNA from The Mouse Liver

In order to confirm whether nano-anatase TiO_2 has damage effects on DNA from the mouse liver, we performed gel electrophoresis (Fig. 6). Figure 6 shows single strand DNA treated with various doses of nano-anatase TiO_2,

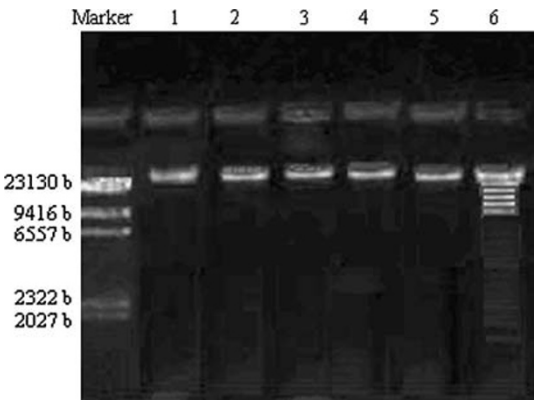

Fig. 6 Assay of complete DNA from liver of mice in various nano-anatase TiO_2 dose groups by agarose gel electrophoresis. *1* Control; *2* 5 mg/kg body weight nano-anatase TiO_2; *3* 10 mg/kg body weight nano-anatase TiO_2; *4* 50 mg/kg body weight nano-anatase TiO_2; *5* 100 mg/kg body weight nano-anatase TiO_2 and *6* 150 mg/kg body weight nano-anatase TiO_2

suggesting that nano-anatase TiO_2 treatments from 5 to 100 mg/kg body weight did not observe liver DNA cleavage, but by 150 mg/kg body weight nano-anatase TiO_2 treatment, liver DNA generated a classical laddering cleavage in vivo.

Discussion

In this study, the ICR mice were injected with various doses of nano-anatase TiO_2 into abdominal cavity everyday for 14 days. In the 50, 100 and 150 mg/kg body weight nano-anatase TiO_2-treated groups, the higher coefficients of the liver were observed ($P < 0.05$ or $P < 0.01$).

A previous study showed that when a fixed high dose of 5 g/kg body weight of nano-TiO_2 suspensions was administrated by a single oral gavage, the coefficients of liver after 2 weeks were significantly increased [1], demonstrating that nano-TiO_2 in higher dose had serious toxicity to the mouse liver. Our studies showed that titanium contents in the liver DNA of mice were gradually elevated with increasing injection doses of nano-anatase TiO_2, which were closely related to the coefficients of the liver of mice. Our previous work showed that the order of the titanium accumulation in the organs of mice was liver > kidneys > spleen > lung > brain > heart, the liver function was damaged [8]. The study suggested that, after entering the animals, nano-anatase TiO_2 was accumulated in DNA of the mouse liver.

The absorbance decreasing effect can be used as an evidence that there exists an interaction model of binding between metal ions and DNA base pairs or nucleotide, i.e., metal ions can coordinate into DNA base pairs and bind to nucleic acids [19, 20]. The experimental results proved that the $\pi \rightarrow \pi^*$ transitions of DNA at 260 nm showed an intensity decrease with increasing doses of nano-anatase TiO_2, which supports the notion that there exists an interaction model of binding, i.e., a strong π-stacking interaction between Ti^{4+} and DNA base pairs [19, 20]. Ti^{4+} can insert into DNA base pairs and bind to nucleotide. Our results are also consistent with the previous studies on the effects of other heavy metal ions on DNA [21–23].

X-ray absorption spectroscopy (XAS) has been proved to be a very powerful technique to detect the local structure around specific elements. The EXAFS contains information of local atomic arrangement for each absorber atom, as described in theoretical formula based on the single-scattering contribution to XAFS. The X-ray fluorescence excitation XAS warrants detection of low concentrations of transition metals presented in metalloenzyme and DNA systems [22–25]. In order to investigate the direct effects of nano-anatase TiO_2 on DNA, we used X-ray absorption technique to study the coordination structure at Ti sites in Ti^{4+}–DNA from the 150 mg/kg body weight nano-anatase TiO_2-treated liver of mice. Our data showed that Ti was bound with three oxygen or nitrogen atoms on DNA in its first shell, and the second shell was two phosphorous atoms, proving that nano-anatase TiO_2 could be bound with the oxygen or phosphorous atoms of nucleotide, and nitrogen atoms of base pairs in DNA.

To further investigate the evidence for interaction of nano-anatase TiO_2 with DNA from the liver of mice, DNA conformation was studied using CD technique. We found that, in the 50, 100 and 150 mg/kg body weight doses of nano-anatase TiO_2, the positive bands at 220 and 272 nm increased and red shifted, and the negative bands at 210 and 244 nm decreased and red shifted, indicating that the transformation from A conformation to B conformation was generated with increasing winding of the DNA helix by rotation of the bases, and nano-anatase TiO_2 caused the shrink of DNA molecule structure [26, 27] herein produced an obvious change of the secondary structure. It was consistent with absorption spectra with respect to this change. The changes of DNA conformation might interfere with the genetic information transmission of DNA and induced inflammatory response of liver consequently [28].

By studying the interaction between nano-anatase TiO_2 and DNA, many previous in vitro studies proved that indirect interaction is associated with oxidative damage to DNA. Being a proven photocatalyst, nano-TiO_2 is capable of undergoing electron transfer reactions under ultraviolet light. For instance, the electron was excited and transferred then photogenerated electron-holes in nano-TiO_2; the electron-holes are reduced when the electron is captured by other molecule, while it is oxidized when itself was captured [29]. In the aqueous environments, nano-TiO_2 would produce hydroxy radical, and hydroxy could react with DNA, producing 8-hydroxy guanosine, which resulted in DNA cleavage and oxidative damage under UVA illumination [30, 31]. Dunford et al. [13] reported that sunlight-illuminated nano-TiO_2 catalyzed DNA damage in both in vitro and human cells. They also used nano-TiO_2 samples extracted from sunscreens to attack PBII DNA under the ultraviolet light between 300 and 400 nm, and relaxed standards and cleavage were observed [18]. Wamer et al. [14] irradiated calf thymus DNA in nano-TiO_2 solutions with UVA radiation in vitro and found the generation of 8-oxo-7 and 8-dihydro-2 *-deoxyguanosine (8-oxodG) in DNA. Ashikaga et al. indicated that supercoiled pBR 322 DNA was formed to open-circular DNA with 5 J/cm^2 of UVA in the presence of TiO_2. The studies mentioned above about DNA effects were carried out both in vitro and under light. The present article proved that nano-anatase TiO_2 caused the changes of DNA conformation in the liver of mice, and we also clearly observed the DNA ladder in liver by agarose gel electrophoresis from the 150 mg/kg body weight nano-anatase TiO_2-treated group, showing that after entering the animals, nano-anatase TiO_2 can cause hepatocyte apoptosis in vivo. The previous study used TEM to observe ultrastructure changes of hepatocyte of the mouse liver tissue, presenting significantly hepatocyte tumescent mitochondria, vacuolization and apoptosis body from the 100 and 150 mg/kg body weight nano-anatase TiO_2-treated groups [28]. Wang et al. observed that the hydropic degeneration around the central vein was prominent and the spotty necrosis of hepatocyte in the liver tissue of female mice postexposure 2 weeks to the 5 g/kg body weight 80 nm and fine TiO_2 particles [1]. Ma et al. [28] indicated that intraperitoneal injection of higher doses of nano-anatase TiO_2 can induce histopathological changes of liver,

including congestion of vascellum, prominent vasodilatation, wide-bound basophilia and focal ischemia. The mechanism of DNA cleavage and hepatocyte apoptosis in vivo caused by nano-anatase TiO_2 was attributed to the significant accumulation of reactive oxygen species in liver of mice [32].

Taken together, we speculate that the combination of nano-anatase TiO_2 with DNA, which is similar to hepatovirus, might cause the inflammatory cascade of the mouse liver, and the alteration of DNA secondary structure in mice caused by nano-anatase TiO_2 might result in the changes of genetic information transmission, and various inflammatory responses, these still need to be confirmed by further study.

Conclusion

The results of experimental study showed that nano-anatase TiO_2 increased the coefficient of the liver of mice and was accumulated in liver DNA. By various spectral methods, we demonstrated that nano-anatase TiO_2 could be inserted into DNA base pairs, bind to DNA nucleotide and alter the secondary structure of DNA. And gel electrophoresis showed that higher dose of nano-anatase TiO_2 did cause liver DNA cleavage and hepatocyte apoptosis in mice.

Acknowledgments This work was supported by the National Natural Science Foundation of China (grant no. 30901218) and by the Medical Development Foundation of Suzhou University (grant no. EE120701) and by the National Bringing New Ideas Foundation of Student of China (grant no. 57315427, 57315927).

References

1. J.X. Wang, G.Q. Zhou, C.Y. Chen, H.W. Yu, T.C. Wang, Y.M. Ma, G. Jia, Y.X. Gao, B. Li, J. Sun, Y.F. Li, F. Jia, Y.L. Zhaso, Z.F. Chai, Acute toxicity and biodistribution of different sized titanium dioxide particles in mice after oral administration. Toxicol. Lett. **168**, 176–185 (2007)
2. J.S. Brown, K.L. Zeman, W.D. Bennett, Ultrafine particle deposition and clearance in the healthy and obstructed lung. Am. J. Respir. Crit. Care Med. **166**, 1240–1247 (2002)
3. W.G. Kreyling, M. Semmler, F. Erbe, P. Mayer, S. Takenaka, H. Schulz, G. Oberdorster, A. Ziesenis, Translocation of ultrafine insoluble iridium particles from lung epithelium to extrapulmonary organs is size dependent but very low. J. Toxicol. Environ. Health A **65**, 1513–1530 (2002)
4. G. Oberdoerster, Z. Sharp, V. Atudorei, A. Elder, R. Gelein, W. Kreyling, C. Cox, Translocation of inhaled ultrafine particles to the brain. Inhal. Toxicol. **16**, 437–445 (2004)
5. G. Oberdörster, E. Oberdörster, J. Oberdörster, Nanotoxicology: an emerging discipline evolving from studies of ultrafine particles. Environ. Health Perspect. **113**, 823–839 (2005)
6. J. Muller, F. Huaux, N. Moreau, P. Misson, J.F. Heilier, M. Delos, M. Arras, A. Fonseca, J.B. Nagy, D. Lison, Respiratory toxicity of multi-wall carbon nanotubes. Toxicol. Appl. Pharmacol. **207**, 221–231 (2005)
7. H.W. Chen, S.F. Su, C.T. Chien, W.H. Lin, S.L. Yu, C. Chou, C. Chen, J.W. Jeremy, P.C. Yang, Titanium dioxide nanoparticles induce emphysema-like lung injury in mice. FASEB J. **20**, 1732–1741 (2006)
8. H.T. Liu, L.L. Ma, J.F. Zhao, J. Liu, J.Y. Yan, J. Ruan, F.S. Hong, Biochemical toxicity of nano-anatase TiO_2 particles in mice. Biol. Trace Elem. Res. **129**(1), 170–180 (2009)
9. G. Oberdörster, J.N. Finkelstein, C. Johnston, Acute pulmonary effects of ultrafine particles in rats and mice. Res. Rep. Health EffInst. **96**, 5–74 (2000)
10. F. Afaq, P. Abidi, R. Matin, Q. Rahman, Cytotoxicity, pro-oxidant effects and antioxidant depletion in rat lung alveolar macrophages exposed to ultrafine titanium dioxide. J. Appl. Toxicol. **18**, 307–312 (1998)
11. B. Gonzalez-Flecha, Oxidant mechanisms in response to ambient air particles. Mol. Aspects Med. **25**, 169–182 (2004)
12. P.S. Vinzents, P. Mfiler, M. Sfiensen, L.E. Knudsen, O. Hertel, F.P. Jensen, B. Schibye, S. Loft, Personal exposure to ultrafine particles and oxidative DNA damage. Environ. Health Perspect. **113**, 1485–1490 (2005)
13. R. Dunford, A. Salinaro, L. Cai, N. Serpone, S. Horikoshi, H. Hidaka, J. Knowl, Chemical oxidation and DNA damage catalysed by inorganic sunscreen ingredients. FEBS Lett. **418**, 87–90 (1997)
14. W.G. Wamer, J.J. Yin, R.R. Weiet, Oxidative damage to nucleic acids photosensitized by titanium dioxide. Free Radic. Biol. Med. **23**(6), 851–858 (1997)
15. T. Ashikaga, M. Wada, H.K. Obayashi, M. Mori, Y.K. Katsumura, H. Fukui, S. Kato, M. Yamaguchi, T. Takamatsu, Effect of the photocatalytic activity of TiO_2 on plasmid DNA. Mutat. Res. **466**, 1–7 (2000)
16. K. Hirakawa, M. Mori, M. Yoshida, S. Oikawa, S. Kawanishi, Photo-irradiated titanium dioxide catalyzes site specific DNA damage via generation of hydrogen peroxide. Free Radic. Res. **38**(5), 439–447 (2004)
17. P. Yang, C. Lu, N. Hua, Y. Du, Titanium dioxide nanoparticles co-doped with Fe^{3+} and Eu^{3+} ions for photocatalysis. Mater. Lett. **57**, 794–801 (2002)
18. A.L. Ankudinov, B. Ravel, J.J. Rehr, S.D. Conradson, Real-space multiple- scattering calculation and interpretation of x-ray-absorption near-edge structure. Phys. Rev. B **58**, 7565 (1998)
19. M.N. Yoshioka, H. Inoue, DNA binding of iron(II) mixed-ligand complexes containing 1, 10-phenanthroline and 4, 7-diphenyl-1, 10-phenanthroline. J. Inorg. Biochem. **77**, 239–247 (1999)
20. J.X. Lu, G.Z. Zhang, Z.N. Huang, P. Zhao, Study on the mechanism of the interaction between mercaptopurine metal complexes and calf thymus DNA. Acta Chimi. Sin. **60**(6), 967–972 (2002). (in Chinese)
21. M.P. Jose, I.M. Ana, M.A. Alfonso, N. Paloma, A. Carlos, S. Pilar, Synthesis and characterization of complexes of *p*-isopropyl benzaldehyde and methyl 2-pyridyl ketone thiosemicarbazones with Zn(II) and Cd(II) metallic centers. Cytotoxic activity and induction of apoptosis in Pam-ras cells. J. Inor. Biochem. **75**, 255–261 (1999)
22. F.S. Hong, C. Wu, C. Liu, K. Wu, F.Q. Gao, F. Yang, Interaction mechanism between Cd^{2+} ions and DNA from kidney of silver crucian carp. Biol. Trace Elem. Res. **110**, 33–44 (2006)
23. F.S. Hong, C. Wu, C. Liu, L. Wang, F.Q. Gao, F. Yang, J.H. Xu, T. Liu, Y.N. Xie, Z.R. Li, Direct interaction between lead ions and DNA from kidney of silver crucian carp. Chemosphere **69**, 1442–1446 (2007)
24. F.S. Hong, L. Wang, K. Wu, X.F. Wang, Y. Tao, Effect of Pb^{2+} on RNase activity and its structure. Acta Chimi. Sin. **61**(1), 117–121 (2003)

25. C. Liu, F.S. Hong, K. Wu, H.B. Ma, X.G. Zhang, C.J. Hong, C. Wu, F.Q. Gao, F. Yang, L. Zheng, Mechanism of Nd3 + ion on increasing carboxylation activity of ribulose-1, 5-bisphosphate carboxylase/oxygenase of spinach. Biochem. Biophys. Res. Comm. **342**(1), 36–43 (2006)
26. M.J. Clarke, B. Jansen, K. Marx, Biochemical effects of binding $[(H_2O)(NH_3)_5Ru^{II}]^{2+}$ to DNA and oxidation to $[(NH_3)_5Ru^{II}]_n$-DNA. Inorg. Chim. Acta **124**, 13 (1986)
27. Z.X. Lu (ed.), *Application of circular dichroism and rotatory dispersion in molecular Biology* (Science Press, Beijing, 1992). (in Chinese)
28. L.L. Ma, J.F. Zhao, J. Wang, Y.M. Duan, J. Liu, N. Li, H.T. Liu, J.Y. Yan, J. Ruan, F.S. Hong, The acute liver injury in mice caused by nano-anatase TiO_2. Nanosacle Res. Lett. (2009, in press). doi 10.1007/s11671-009-9393-8
29. N. Serpone, *Kirk–Othmer Encyclopedia of Chemical Technology*, vol. 18 (Wiley-Interscience, New York, 1996), pp. 820–837
30. H. Zheng, P.C. Maness, D.M. Blake, J. Wolfrum, J. Edward, Bactericidal mode of titanium dioxide photocatalysis. J. Photochem. Photobiol. A Chem. **130**, 163–170 (2000)
31. S. Kayano, W. Toshiya, H. Kazuhito, Studies on photokilling of bacteria on TiO_2 thin film. J. Photochem. Photobiol. A Chem. **156**, 227–233 (2003)
32. H.T. Liu, L. Ma, J.F. Zhao, J. Liu, J.Y. Yan, J. Ruan, F.S. Hong, Toxicity of nano-anatase TiO_2 to mice: liver injury, oxidative stress. Toxicol. Environ. Chem. (2009 in press). doi 10.1080/02772240902732530